

Photoluminescence and polarized photodetection of single ZnO nanowires

Zhiyong Fan, Pai-chun Chang, and Jia G. Lu^{a)}

Department of Chemical Engineering and Materials Science & Department of Electrical Engineering and Computer Science, University of California, Irvine, California 92697

Erich C. Walter and Reginald M. Penner

Department of Chemistry, University of California, Irvine, California 92697

Chien-hung Lin and Henry P. Lee

Department of Electrical Engineering and Computer Science, University of California, Irvine, California 92697

(Received 15 July 2004; accepted 27 October 2004)

Single crystal ZnO nanowires are synthesized and configured as field-effect transistors. Photoluminescence and photoconductivity measurements show defect-related deep electronic states giving rise to green-red emission and absorption. Photocurrent temporal response shows that current decay time is significantly prolonged in vacuum due to a slower oxygen chemisorption process. The photoconductivity of ZnO nanowires is strongly polarization dependent. Collectively, these results demonstrate that ZnO nanowire is a remarkable optoelectronic material for nanoscale device applications. © 2004 American Institute of Physics. [DOI: 10.1063/1.1841453]

Low dimensional systems such as quantum dots, nanotubes, and nanowires have fascinating, and technologically useful, optical and electrical properties. Studies on these systems advance our knowledge on low dimensional physics and chemistry; while simultaneously providing the possibility for the development of nanoscale electronics and optoelectronics. Nanostructures composed of ZnO nanowires (NWs) are being intensively investigated because they possess a combination of attractive optical,¹ mechanical,² and magnetic properties.³ ZnO NWs have been evaluated for potential applications as UV laser,⁴ light-emitting diodes,⁵ and UV photodetectors.^{6,7} However, the effort of fabricating and characterizing single ZnO NW phototransistor, an important component for building optoelectronic circuit, has not been reported. Photoconduction of mass grown NWs between electrodes could not demonstrate polarization dependence, which is a unique property of quasi-one-dimensional system. In this letter, we report optical properties of single ZnO NWs configured as field-effect transistors (FETs), including photoluminescence (PL), and polarization-dependent photoconductivity. The PL measurements showed both near-band edge emission near 3.37 eV and green-red emission from native defects. Photoconductivity was also observed both at the band-edge and at energies corresponding to the deep trap states as seen in PL spectra. The photocurrent varies as a function of $\cos^2 \theta$, where θ is the angle between the polarization of incident light and long axis of the nanowire.

ZnO NWs were synthesized by a vapor trapping chemical vapor deposition method.⁸ Field emission scanning electron microscopy (FE-SEM) [Fig. 1(a)] shows as-synthesized NWs are 30–150 nm in diameter and $\sim 40 \mu\text{m}$ in length. Transmission electron microscopy (TEM) [Fig. 1(b)] and selective area electron diffraction show that NWs are single crystalline and the growth direction is [001].

Individual ZnO NWs were configured as FETs on *p*-type degenerately doped silicon substrate capped with 500-nm-

thick SiO₂ layer. The top inset of Fig. 1(c) shows an atomic force microscope image of such a device. Electrical transport properties were studied at room temperature. Figure 1(c) shows the I - V curves for a FET at different gate voltages. The conductance of the NW increases with gate voltage in accordance with *n*-type semiconducting behavior. This *n*-type behavior is mainly attributed to Zn interstitials and oxygen vacancies generated during the synthesis process.^{8–10} Furthermore, transconductance is obtained at 0.4 V drain-source bias (V_{ds}) and shown in the bottom inset of Fig. 1(c). A carrier mobility of 26.3 cm²/V s is estimated

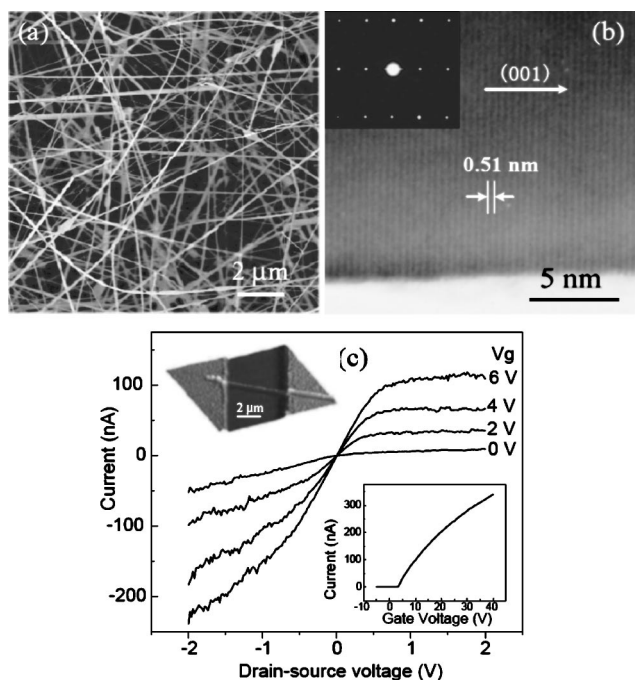


FIG. 1. (a) SEM image of as synthesized ZnO NWs. (b) High resolution TEM image with selected area electron diffraction pattern (inset) of a ZnO NW. (c) I - V curves for a ZnO NW FET at different gate voltages. Top inset: AFM image of the NW FET. Bottom inset: transconductance of NW FET vs gate voltage.

^{a)} Author to whom correspondence should be addressed; electronic mail: jglu@uci.edu

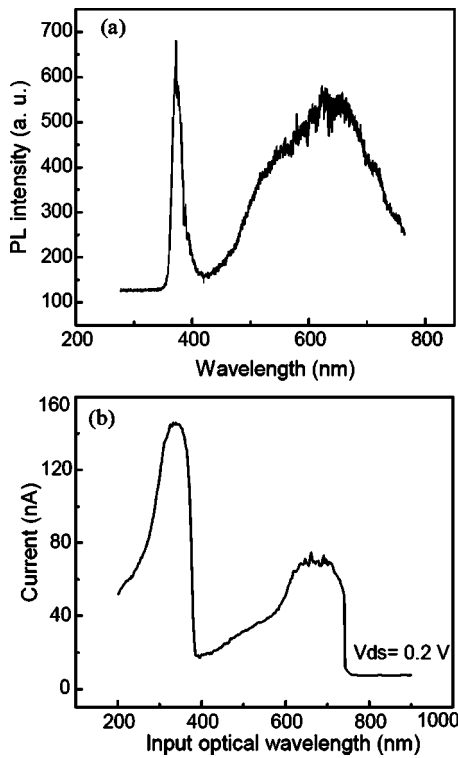


FIG. 2. (a) The PL of a ZnO NW excited with 351 nm UV laser. (b) The photoconductivity of a ZnO NW obtained at 0.2 V drain-source bias (V_{ds}).

using the relationship¹¹ $\mu_e = (dI/dV_g) / (2\pi\epsilon\epsilon_0 V_{ds} / L \ln(2h/r))$, where $dI/dV_g = 6.87 \times 10^{-9}$ A/V is extracted from the linear region of the transconductance, $\epsilon = 3.9$, $L = 10.3 \mu\text{m}$ the NW channel length, $h = 500$ nm gate oxide layer thickness, and $r = 40$ nm nanowire radius. The obtained electron mobility in ZnO NW is much higher than that of high mobility ZnO thin film transistor.¹²

The PL of ZnO has been extensively studied for its potential optical applications.³⁻⁵ PL spectra for single ZnO NWs were acquired with an Ar⁺ ion laser (351nm, 50 mW). A typical spectrum [Fig. 2(a)] shows two PL bands. The first luminescence band centered at 380 nm (3.26 eV) indicates

the near-band-edge (3.37 eV) emission and free-exciton peak of ZnO. The second green-red luminescence band centered at 650 nm (1.92 eV) is also observed, which is caused by native defect levels within the band gap, such as single and double ionized oxygen vacancies.^{13,14} The single NW photoconductivity spectrum is obtained using a monochromated xenon arc lamp source that covers a range from 200 to 900 nm. The result of photoconductivity [Fig. 2(b)] shows similar spectroscopic feature as the PL spectrum. Strong absorption at 380 nm and at longer wavelengths (400–740 nm) are observed. The broad photoconductivity peak at 340 nm is reminiscent of semiconductor of the electronic density of states near the conduction band edge.

The detection of UV light (365 nm) using ZnO NWs has been studied and photoresponse to longer wavelength has not been reported.⁶ In contrast, our PL and photoconductivity results for ZnO NWs indicate that defect-related deep electronic states confer sensitivity to visible light (400–750 nm). Figure 3(a) shows with 633 nm He-Ne laser illumination (~ 0.2 W/cm²), the conductance of NW increased from 13.1 nS in dark to 73.4 nS at 2 V drain-source bias. Laser illumination also affects the transconductance as shown in the inset of Fig. 3(a), causing a shift in the threshold gate voltage from +0.6 to -2.0 V. Since one-dimensional electron concentration is expressed as $n = (C/L)(V_{gt}/e)$,¹¹ where $C/L \approx 2\pi\epsilon\epsilon_0 / \ln(2h/r)$ is the capacitance per unit length with respect to the back gate, and V_{gt} is the magnitude of the threshold gate voltage. Therefore, from the shift in gate voltage, the change in the electron concentration, Δn , is estimated as $\Delta n = (\Delta V_{gt}/e)(2\pi\epsilon\epsilon_0 / \ln(2h/r))$. Using $\Delta V_{gt} = 2.6$ V and $r = 43$ nm, Δn is approximately 1.1×10^7 cm⁻³. Due to illumination, transconductance is observed to decrease from 2.9 to 2.6×10^{-9} A/V; as a result, electron mobility drops slightly from 23.4 to 21.0 cm²/V s. The mobility decrease is attributed to the enhanced electron–electron scattering at higher carrier concentration.

The intensity dependence of the photocurrent was studied with 633 nm laser. As shown in Fig. 3(b), the relationship between photocurrent and input optical power obeys power law dependence, i.e., $I = A \times P^{0.43}$ where A is a constant. This

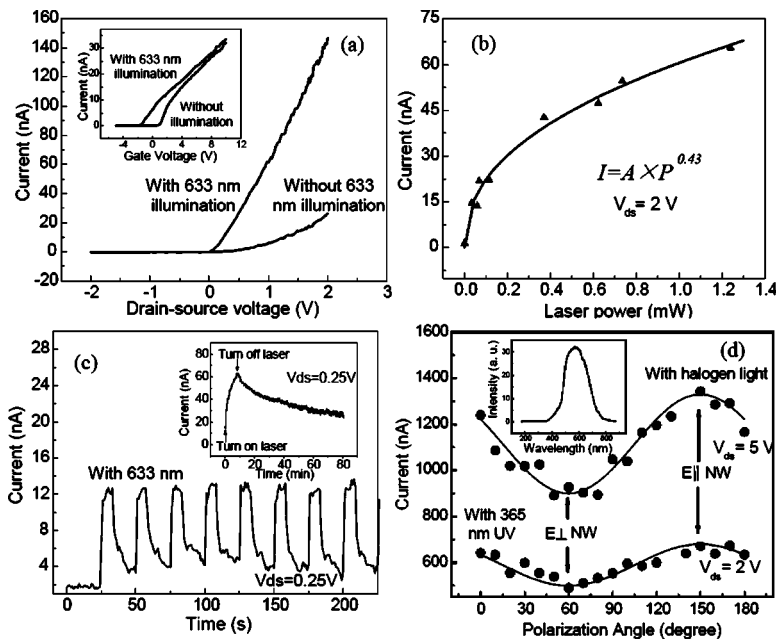


FIG. 3. (a) I - V curves and transconductance of a ZnO NW with and without 633 nm laser illumination. (b) Power law dependence of photocurrent on input optical power. The red curve is a power law fitting showing an exponent of 0.43. (c) The time domain measurements of photo-response to 633 nm laser in air and 10^{-3} Torr (inset). (d) Photocurrent as a function of the light polarization angle for both UV (bottom) and visible light (top). The inset plot shows a spectrum of halogen light source.

nonlinear behavior fits well with the theory of photo-response which gives a power law dependence with an exponent of 0.5. This is a result of the finite density of deep donor levels compared with the flux of incident photons.¹⁵

Time-resolved measurements of photo-response to pulsed 633 nm laser were conducted and shown in Fig. 3(c). The results show ZnO NW FET can be reversibly turned “on” and “off” by switching illumination. Photocurrent decay process is observed to be significantly affected by oxygen (O₂) ambient. If photocurrent decay time T_d is defined as the time for current to drop to I_{\max}/e ,¹⁶ T_d is estimated to be 8 s in air. In contrast, the decay time is much longer 10^{-3} Torr vacuum, i.e., $T_d > 1$ Hs shown in the inset of Fig. 3(c). It is known that the surface adsorbed oxygen significantly affects the photoresponse of ZnO films and NWs.^{7,17–19} Oxygen is chemisorbed to ZnO surface at vacancy sites, forming O₂⁻ and resulting in a surface charge depletion layer thus leading to a reduction in the electrical conductivity.²⁰ Upon illumination, photoexcited holes discharge the adsorbed O₂⁻ ions through surface electron–hole recombination, while the photoexcited electrons significantly increase the conductivity.^{4,19} When illumination is switched off, oxygen chemisorption process dominates and assists photoconductivity relaxation. As a result of this scenario, the photocurrent relaxation dynamics is strongly affected by the ambient O₂ partial pressure. Due to a much lower O₂ pressure in vacuum, the relaxation time is expected to be much longer than that in air, as observed in the experiment. For quasi-one-dimensional NWs where the radius is comparable to the Debye length, this surface effect becomes more pronounced in the charge carrier dynamics.

The photoconductance of ZnO NWs is sensitive to the polarization of the incident illumination. Specifically, the photocurrent is proportional to $\cos^2 \theta$, where θ is the angle between the polarization of incident light and long axis of the nanowire. For these measurements, a halogen illuminator (Dolan Jenner 190, 30 W) and a handheld 365 nm UV lamp (entela, 18 W) are used in conjunction with a Glan-Thompson linear polarizer. As shown in Fig. 3(d), photocurrent is maximized when the incident light is polarized parallel to the NW axis and minimized otherwise. This polarized photodetection has also been reported for InP and GaN NWs.^{21,22} When NW diameter is much smaller than wavelength, electric field component of light normal to NW axis is effectively attenuated inside the NW due to confinement. The polarization-dependent behavior can be utilized for realizing broad band high contrast polarizer using arrays of NWs aligned in parallel direction.

Single crystal ZnO nanowires are synthesized and configured as field-effect transistors. Photoluminescence and

photoconductivity studies show green-red emission related to deep-level states in addition to band-to-band transition. Photocurrent temporal response shows ZnO FET can function as an optoelectronic switch. In addition, the photo-conduction of ZnO NW is observed to strongly depend on the polarization of the incident light. These results indicate that ZnO NW is a promising nanoscale optoelectronic material for visible light as well as UV range applications.

This work was supported by National Science Foundation Grant No. ECS-0306735 and performed at UC, Irvine Integrated Nanosystem Research Facility (INRF). R.M.P. and E.C.W. acknowledge support of this work through NSF No. DMR-0405477.

- ¹X. Wang, C. J. Summers, and Z. L. Wang, *Nano Lett.* **4**, 423 (2004).
- ²X. D. Bai, P. X. Gao, Z. L. Wang, and E. G. Wang, *Appl. Phys. Lett.* **82**, 4806 (2003).
- ³Y. W. Chang, D. B. Wang, X. H. Luo, X. Y. Xu, X. H. Chen, L. Li, C. P. Chen, R. M. Wang, J. Xu, and D. P. Yu, *Appl. Phys. Lett.* **83**, 4020 (2003).
- ⁴P. Yang, H. Yan, S. Mao, R. Russo, J. Johnson, R. Saykally, N. Morris, J. Pham, R. He, and H.-J. Choi, *Adv. Funct. Mater.* **12**, 323 (2002).
- ⁵C. H. Liu, J. A. Zapfen, Y. Yao, X. M. Meng, C. S. Lee, S. S. Fan, Y. Lifshitz, and S. T. Lee, *Adv. Mater. (Weinheim, Ger.)* **15**, 838 (2003).
- ⁶H. Kind, H. Yan, B. Messer, M. Law, and P. Yang, *Adv. Mater. (Weinheim, Ger.)* **14**, 158 (2002).
- ⁷K. Keem, H. Kim, G.-T. Kim, J. S. Lee, B. Min, K. Cho, M.-Y. Sung, and S. Kim, *Appl. Phys. Lett.* **84**, 4376, (2004).
- ⁸P. Chang, Z. Fan, W. Tseng, D. Wang, W. Chiou, J. Hong, and J. G. Lu, *Chem. Mater.* (to be published).
- ⁹Z. Fan, D. Wang, P. Chang, and J. G. Lu, *Appl. Phys. Lett.* (to be published).
- ¹⁰M. Joseph, H. Tabata, H. Saeki, K. Ueda, and T. Kawai, *Physica B* **302–303**, 140 (2001).
- ¹¹R. Martel, T. Schmidt, H. R. Shea, T. Hertel, and Ph. Avouris, *Appl. Phys. Lett.* **73**, 2447 (1998).
- ¹²J. Nishii, F. M. Hossain, S. Takagi, T. Aita, K. Saikusa, Y. Ohmaki, I. Ohkubo, S. Kishimoto, A. Ohtoma, T. Fukumura, F. Matsukura, Y. Ohno, H. Koinuma, H. Ohno, and M. Kawasaki, *Jpn. J. Appl. Phys., Part 2* **42**, L347 (2003).
- ¹³K. Vanheusden, C. H. Seager, W. L. Warren, D. R. Tallan, J. Caruso, M. J. Mampden-Smith, and T. T. Kodas, *J. Lumin.* **75**, 11 (1997).
- ¹⁴U. Schwing and B. Hoffman, *J. Appl. Phys.* **57**, 5372 (1984).
- ¹⁵T. S. Moss, *Photoconductivity in the Elements* (Butterworths Scientific, London, 1952).
- ¹⁶R. H. Bube, *Photoconductivity of Solids* (Wiley, New York, 1960).
- ¹⁷D. H. Zhang and D. E. Brodie, *Thin Solid Films* **261**, 334 (1995).
- ¹⁸S. A. Studenikin, N. Golego, and M. Cocivera, *J. Appl. Phys.* **87**, 2413 (2000).
- ¹⁹H. Geistlinger, *J. Appl. Phys.* **80**, 1370 (1996).
- ²⁰V. E. Henrich, *The Surface Science of Metal Oxides* (Cambridge University Press, New York, 1994).
- ²¹J. Wang, M. S. Gudiksen, X. Duan, Y. Cui, and C. M. Lieber, *Science* **293**, 1455 (2001).
- ²²S. Han, W. Jin, D. Zhang, T. Tang, C. Li, X. Liu, Z. Liu, B. Lei, and C. Zhou, *Chem. Phys. Lett.* **389**, 176 (2004).